Rationally Designed Dehydroalanine (ΔAla)-Containing Peptides Inhibit Amyloid-β (Aβ) Peptide Aggregation

Vijayaraghavan Rangachari,* Zachary S. Davey, Brent Healy, Brenda D. Moore, Leilani K. Sonoda, Bernadette Cusack, Ghulam M. Maharvi, Abdul H. Fauq, Terrone L. Rosenberry
Department of Neuroscience, Mayo Clinic College of Medicine, 4500 San Pablo Road, Jacksonville, FL 32224

Received 6 June 2008; revised 15 January 2009; accepted 16 January 2009
Published online 2 February 2009 in Wiley InterScience (www.interscience.wiley.com). DOI 10.1002/bip.21151

ABSTRACT:

Among the pathological hallmarks of Alzheimer's disease (AD) is the deposition of amyloid-β (Aβ) peptides, primarily Aβ (1–40) and Aβ (1–42), in the brain as senile plaques. A large body of evidence suggests that cognitive decline and dementia in AD patients arise from the formation of various aggregated forms of Aβ, including oligomers, protofibrils and fibrils. Hence, there is increasing interest in designing molecular agents that can impede the aggregation process and that can lead to the development of therapeutically viable compounds. Here, we demonstrate the ability of the specifically designed α,β-dehydroalanine (ΔAla)-containing peptides P1 (K-L-V-F-ΔA-I-ΔA) and P2 (K-F-ΔA-ΔA-ΔA-F) to inhibit Aβ (1–42) aggregation. The mechanism of interaction of the two peptides with Aβ (1–42) seemed to be different and distinct. Overall, the data reveal a novel application of ΔAla-containing peptides as tools to disrupt Aβ aggregation that may lead to the development of anti-amyloid therapies not only for AD but also for many other protein misfolding diseases. © *2009 Wiley Periodicals, Inc. Biopolymers 91: 456–465, 2009.*

Keywords: amyloid aggregation; inhibition; dehydro-alanine; rational design

Additional Supporting Information may be found in the online version of this article.

Correspondence to: Vijayaraghavan Rangachari; e-mail: vijay.rangachari@usm.edu
**Present address*: Department of Chemistry and Biochemistry, University of Southern Mississippi, 118 College Dr #5043, Hattiesburg, MS 39406.

Contract grant sponsor: American Heart Association, National Center
Contract grant number for V.R.: 0535185N

This article was originally published online as an accepted preprint. The "Published Online" date corresponds to the preprint version. You can request a copy of the preprint by emailing the Biopolymers editorial office at biopolymers@wiley.com

INTRODUCTION

Alzheimer's disease (AD) is a progressive and ultimately a fatal neurodegenerative disease that affects the elderly. Brains of patients with AD contain numerous deposits of senile plaques composed mainly of 40- and 42-residue peptides called amyloid-β (Aβ) peptides. Aβ peptides are generated as a result of sequential proteolytic processing of amyloid precursor protein (APP) by β- and γ-secretases.[1] Genetic mutations give rise to early-onset familial AD (FAD), and many of these mutations result in increased production of the longer and more amyloidogenic peptide Aβ(1–42).[2,3] However, considerable evidence suggests that cognitive decline and dementia in AD patients arise from the formation of various soluble forms of aggregated Aβ in addition to the fibrillar deposits in plaques. These forms include oligomers and protofibrils, and recent reports propose that low molecular weight soluble oligomers of Aβ are the primary neurotoxic agents responsible for memory deficits.[4–7] Therefore, there is enormous interest in understanding the formation of neurotoxic Aβ aggregates in the context of developing AD therapeutics.

One straightforward strategy for the development of a therapy for AD is to design inhibitors that can impede or reverse the Aβ aggregation process. Drug design is a time-consuming and expensive endeavor. One of the most time consuming steps is the identification of lead compounds and their optimization. It is estimated that for every 5000 lead compounds, only 1 is successfully tested in clinical trials.[8] Therefore, it is extremely useful to minimize the time and effort in lead compound identification and optimization. In this context, peptides based on amino acid sequences found at points of contact during Aβ—Aβ interaction make

excellent candidates for a lead compound. In such protein-protein interaction cases, different kinds of amino acids (charged and hydrophobic) contribute to the free energy of interaction, and an initial strategy for developing aggregation inhibitors is to examine the interaction interface and synthesize peptides which correspond to the interface sequences. The next step involves the identification of contact residues at the interface. Once the structure of a lead peptide is known, it can be converted to a peptidomimetic or organic compound that conserves the critical interactions required for inhibition. Based on this approach, peptide-based lead compounds have been developed for inhibiting Aβ aggregation.[9–14] One important peptide sequence that illustrates this strategy is the pentapeptide fragment KLVFF, corresponding to residues 16–20 of Aβ, that binds to the identical segment in wild-type Aβ in a stereo-specific manner.[11,15–17] Derivatives and analogs of this pentapeptide have been shown to inhibit Aβ aggregation.[10,12,15,17]

α,β-Dehydro-amino acid residues are known to be strong inducers of specific peptide backbone conformations. Although dehydro-amino acid residues are not coded for translation by ribosomes, their occurrence in nature can be observed sporadically in antibiotic peptides. ΔAla is present in antibacterial peptides including nisin[18] and nosiheptide.[19] However, more interest in these amino acids arises from their ability to generate specific structures as well as their protease resistance, both of which encourage their use in rational molecular design. Design rules using dehydro-residues have been formulated to generate specific peptide secondary structures.[20] Substitution of ΔAla in peptide sequences has been shown to induce extended conformations to the peptide backbone (backbone dihedral angles $[\phi, \psi] = \sim[-180, 180^\circ]$) corresponding to a *trans* orientation.[20,21] These local constraints induced by ΔAla residues can be extended to the entire length of the peptide by inserting ΔAla in appropriate sites. When placed successively $[(\Delta Ala)_n]$, the peptide adopts an extended, planar conformation.[22] Although only a small number of peptide structures containing ΔAla have been reported in the literature (Ref. 20 and references therein), many molecular simulation models also support these structural results and suggest that an extended, planar conformation is the one most preferred by this modified amino acid.[23,24] Moreover, designed ΔAla peptides have been observed to form β-sheets in x-ray structures,[25] supporting their propensity to adopt such secondary structures. We therefore reasoned that, if a heterogeneous complex of Aβ with a ΔAla-containing peptide could be formed by targeting specific areas of Aβ, the resulting induced local conformation would disrupt the nucleation of Aβ aggregation and impair further aggregation.

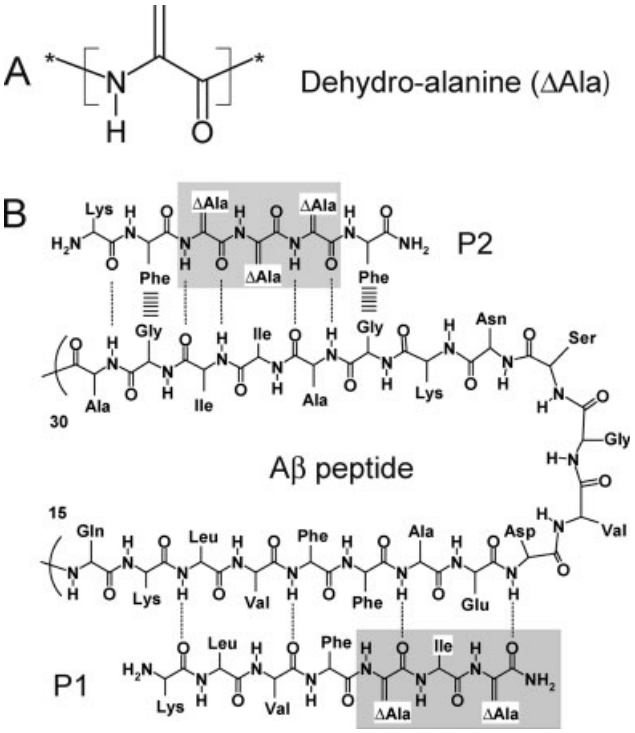

FIGURE 1 Panel A shows the schematic chemical structure of the ΔAla-amino acid residue. Shown in panel B is the schematic structure of residues 15–30 of an Aβ(1–40) or Aβ(1–42) monomer unit in a fibril assembly along with those of peptides P'1 and P2. The functional parts of the designed peptides which contain the ΔAla moiety are shaded in grey. The hypothesized area of interactions of the peptides P1 and P2 with Aβ(1–42) are indicated. Hydrogen bonds are represented as (---) and hydrophobic interactions as (IIIII).

Based on previous reports and existing structural models, we synthesized ΔAla-containing peptides P1 and P2 (Figure 1B) that were designed to interact with two distinct regions of the Aβ peptide, and we determined their ability to inhibit Aβ aggregation. The peptide P1 (K-L-V-F-ΔA-I-ΔA) contained the "KLVF" moiety noted above as a binding or recognition motif and "ΔA-I-ΔA" as a disrupting or functional motif (Figure 1B). We hypothesized that the "ΔA-I-ΔA" motif would disrupt the turn conformation between residues 23 and 29 observed in Aβ fibrils[26] by imposing a linear extended conformation to a segment containing residues 23 and 25. By disrupting the ability of Aβ to adopt this critical turn conformation, we anticipated effective inhibition of Aβ aggregation at an early step. The design of peptide P2 (K-F-ΔA-ΔA-ΔA-F) was based on the observation that peptides containing FxxxF bound to the groove formed by a GxxxG motif (residues G33–G37) in a β-sheet segment of Aβ(1–40) fibrils and impeded aggregation.[14] We reasoned that the planar conformation adopted by the FΔAΔAΔAF motif may enhance the ability of the peptide to bind to the GxxxG groove (Figure 1B) and consequently inhibit

aggregation. Furthermore, because the FxxxF interaction with Aβ(1–40) fibrils is independent of binding orientation,[17] P2 may be able to bind in both parallel and anti parallel orientations, increasing its ability to interact with Aβ. The observations in this manuscript are the first to report the "utility" of dehydro-amino acids in rational design of potentially therapeutic molecules.

MATERIALS AND METHODS

Materials

Aβ(1–42) and peptides P1* (KLVFAIA) and P2*(KFAAAF) were synthesized on preloaded NovaSyn TGA resins (EMD Novabiochem, San Diego, CA) utilizing orthogonal Fmoc solid phase chemistry by the Peptide Synthesis Facility at the Mayo Clinic (Rochester, MN), as previously described.[27] MALDI-TOF mass spectrometry revealed >90% purity of these peptides. SDS, bovine serum albumin, and thioflavin T were procured from Sigma (St. Louis, MO). All other buffers and salts were obtained from Fisher Inc.

Syntheses of ΔAla Peptides

The peptides P1 and P2 were synthesized by the following protocol modified from a previously reported procedure.[22]

Synthesis of P1 (Scheme 1)

(a) Tert-butyl 3,3′-((2S,5S,8S,11S,14S)-5,8,11-tris((benzyloxycarbonylamino)methyl)-14-((S)-2,6-bis(tert-butoxycarbonylamino)hexanamido)-2-carbamoyl-4,7,10,13-tetraoxo-3,6,9,12-tetraazapentadecane-1,15-diyl)bis(1H-indole-1-carboxylate) **2.** PL-Sieber resin (Polymer laboratories Inc, Amherst, MA) (403 mg, 0.62 mmol/g of Fmoc-blocked amino groups) was placed in a clamped glass filter funnel with a glass frit. A slow, steady flow of dry nitrogen was allowed to pass through the resin from the lower end via a piece of Tygon tubing. Fmoc on the Sieber resin was removed by shaking with 10 ml of 20% piperidine (PIP) in dimethylformamide (DMF) under dry nitrogen for 15 min and the liquid phase drained. This process was repeated once. After washing the deprotected resin with DMF (10 ml × 5), the first Fmoc-amino acid was coupled to the resin by addition of a clear preformed reagent cocktail prepared by vortexing a mixture of 2.2 ml of O-benzotriazole-N,N,N′,N′-tetramethyl-uronium-hexafluorophosphate (HBTU)/1-hydroxybenzotriazole (HOBT) (1 mmol each) in DMF, solid Fmoc (Boc)-protected amino acid (1 mmol) or Fmoc-benzyloxycarbonyl (Cbz)-diaminopropanoic acid (DAP), and 348 μl diisopropylethylamine (DIPEA) (2 mmol). The resulting suspension was shaken under nitrogen for 1 h at room temperature. Completion of the reaction was monitored after each coupling with ninhydrin reagent (Kaiser test) and the coupling was repeated if needed. The liquid residue was drained off with nitrogen pressure and the resin was washed with dry DMF (8 ml × 4). The Fmoc amine protecting group on the newly added amino acid was removed with 20% PIP as described above. This process of Fmoc removal and coupling was repeated with the remaining Fmoc-protected amino acids and Fmoc-DAP in the peptide sequence. After final coupling with Boc-Lys(Boc) and thorough washing first with DMF (10 ml × 3) and then with dichloromethane (DCM) (10 ml × 4), the resin-bound tert-butoxycarbonylation (Boc)- and Cbz-protected peptide *1* was cleaved off the resin by wrist action shaking with 10 ml of 2% trifluoracetic acid (TFA)/DCM under nitrogen and the extract drained. The resin was thoroughly washed with DCM (10 ml × 4). The extracts were combined and neutralized with solid $NaHCO_3$ and filtered. This process was repeated one more time. The two extracts were combined and the volatiles were removed under rotary evaporation to afford the crude protected peptide, which on purification with silica gel chromatography (eluting with 2% MeOH/DCM) produced 300 mg (76%) of the pure protected peptide *2* as a yellowish gummy solid.

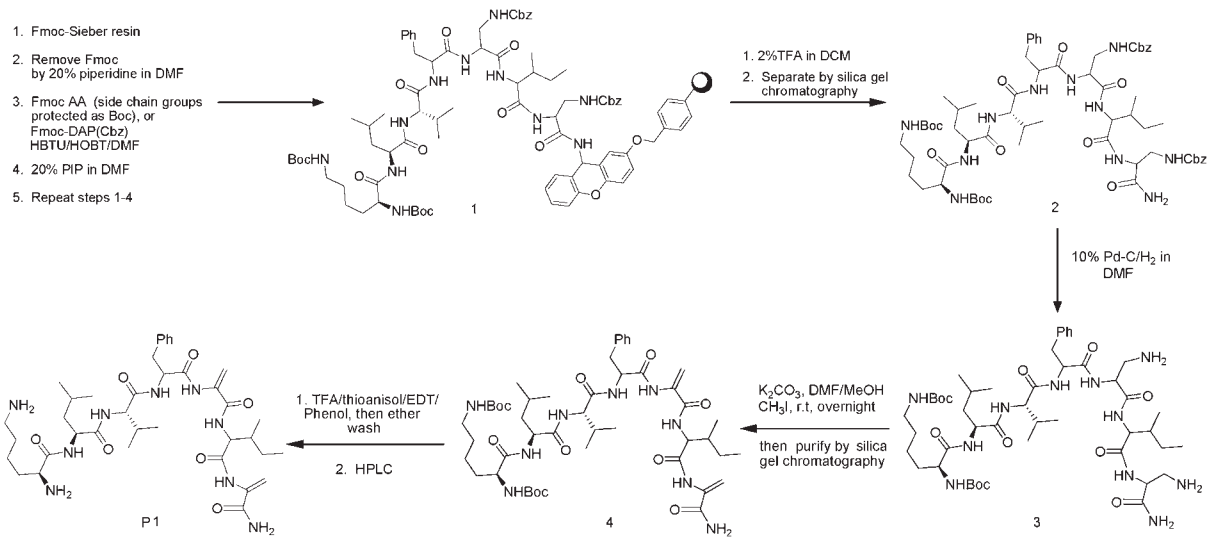

SCHEME 1 Synthesis of peptide P1 by solid/solution-phase protocol.

(b) Tert-butyl 3,3′-((2S,5S,8S,11S,14S)-5,8,11-tris(aminomethyl)-14-((S)-2,6-bis(tert-butoxycarbonylamino)hexanamido)-2-carbamoyl-4,7,10,13-tetraoxo-3,6,9,12-tetraazapentadecane-1,15-diyl)bis(1H-indole-1-carboxylate) **3.** The purified Boc- and Cbz-protected peptide *2* (300 mg) was dissolved in DMF (3 ml). 10% Pd-C (180 mg) was added and the mixture was hydrogenated under 1 atm (balloon) pressure for 1 h. The progress of the reaction was monitored by electrospray mass spectrometry (ESI-MS). After filtering the reaction mixture over Celite, the solvent was evaporated under high vacuum. This product *3* was taken to the next step without purification.

(c) Tert-butyl 3,3′-((2S,14S)-14-((S)-2,6-bis(tert-butoxycarbonylamino)hexanamido)-2-carbamoyl-5,8,11-trimethylene-4,7,10,13-tetraoxo-3,6,9,12-tetraazapentadecane-1,15-diyl) bis(1H-indole-1-carboxylate) **4.** This reaction is a crucial step in the formation of ΔAla, which occurs via exhaustive methylation of a DAP residue followed by *β*-elimination as previously reported.[22] To a solution of Cbz-deprotected peptide *3* (149 mg, 127 *μ*mol) in 1:3 MeOH/DMF (10 ml) was added CH_3I (0.31 ml, 4.9 *μ*mol) and $KHCO_3$ (246 mg, 2.46 *μ*mol), and the reaction mixture was stirred overnight at room temperature under nitrogen. Upon completion of the reaction (TLC monitoring), ethylacetate (EtOAc) (50 ml) was added to the reaction mixture. The precipitated insoluble material was filtered off, and the filtrate was concentrated under reduced pressure. The residue was taken up in EtOAc (50 ml), washed with water (10 ml × 3), 10% citric acid in water (10 ml × 3), saturated $NaHCO_3$ solution, and finally in brine (10 ml × 3), and then it was dried over $MgSO_4$, filtered and evaporated under reduced pressure below 25°C to afford the target compound **4** as a yellow gummy solid. The product was purified by eluting with 2–3% MeOH/DCM on silica gel (yield 61 mg, 42%). The silica gel purification was found to be important for clean conversion to the final product **P1** in the next step.

(d) (S)-N-((2S,14S)-2-((1H-indol-3-yl)methyl)-1-amino-15-(1H-indol-3-yl)-5,8,11-trimethylene-1,4,7,10,13-pentaoxo-3,6,9,12-tetraazapentadecan-14-yl)-2,6-diaminohexanamide **P1**. The Boc-protected peptide *4* was dissolved in 3 ml of 85% TFA, 5% H_2O, 5% 1,2-ethanedithiol (EDT), 2.5% thioanisol, and 2.5% phenol in a glass vial, and the reaction mixture was allowed to stir for 1 h at room temperature under nitrogen. The TFA was removed under reduced pressure and the residue was treated with cold ether. The resulting precipitate was isolated by centrifugation with cold ether wash. The crude residue was finally purified by reverse phase HPLC using 0.1% aqueous TFA and 80% aqueous acetonitrile containing 0.1% TFA. The collected fractions were pooled and lyophilized to furnish a pale yellow gummy solid that was characterized by ESI-MS; yield 27 mg, 69%. ESI-MS for P1 showed a m/z peak at 757.5 (M+1) (see Figure 2).

Synthesis of P2

The above procedure was also followed for the synthesis of $KF(\Delta A)_3F$ (P2) with similar results. ESI-MS for P2 showed a m/z peak at 647.5 (M+1) (see Figure 2).

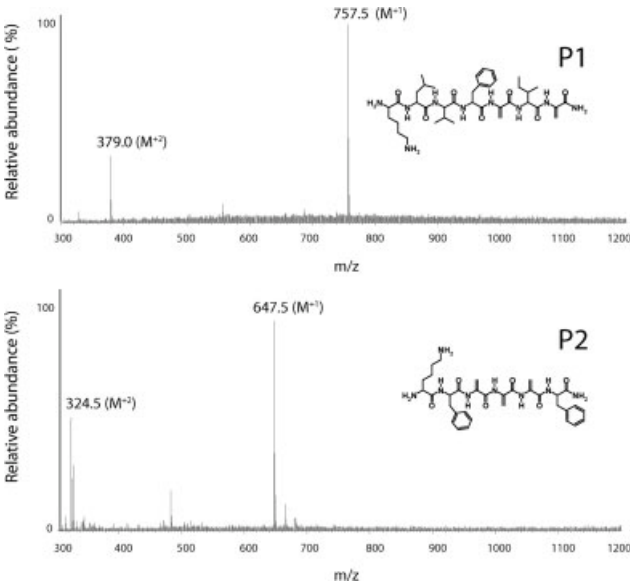

FIGURE 2 Characterization of synthesized peptides. ESI mass spectrometry was conducted as outlined in the Material and Methods, and the spectra of the two synthesized peptides, P1 and P2, show the M^{+1} and M^{+2} peaks.

BCA Assay for Determining Peptide Concentrations

Protein standards were made using bovine serum albumin stock. Assays were performed with three concentrations of peptides P1 and P2 in triplicate using the protein assay kit (Pierce Inc, Rockford, IL) as per manufacturer's specifications.

Mass Spectrometry

Mass Spectrometry (MS) analyses of the peptides were performed on a Thermo Electron Corp (San Jose, CA) ESI LCQ DECA XP Plus ion trap mass spectrometer. Peptides were directly infused with the Nanomate 100 attachment (Advion Biosciences, Ithaca, NY). The mass spectrometer was tuned using angiotensin I peptide in the positive ion mode and the following settings were used for analysis: capillary temperature 160°C, capillary voltage 59.5 V. The peptides were dissolved in CH_3CN:H_2O:HCOOH (50:50:0.2%) at concentrations of 1–10 pmol/*μ*l.

Size Exclusion Chromatography

Column preparation and use generally were described previously.[28] In brief, samples (0.5–1.0 ml) were loaded on to a 1 × 30 cm^2 Superdex 75 HR 10/30 column (Amersham Pharmacia) attached to either an AKTA FPLC or a Pharmacia LKB system. The column was pre-equilibrated in 20 mM Tris-HCl (pH 8.0) at 25°C and run at a flow rate of 0.5 ml/min. One minute fractions were collected.

Preparation of A*β*(1–42) Monomers and Fibrils

Lyophilized stocks of A*β*(1–42) were stored at −80°C desiccated. The peptide was dissolved at 0.5–2.0 m*M* in 30 m*M* NaOH[29] 15 min prior to Size Exclusion Chromatography (SEC) on Superdex 75. Peptide integrity after SEC was again confirmed by MALDI-TOF mass spectrometry. Monomeric A*β*(1–42) was used within one day of SEC

purification in all experiments. Concentrations of Aβ were determined by UV absorbance with a calculated extinction coefficient of 1450 cm^{-1} M^{-1} at 276 nm. Fibrils were prepared by incubating purified Aβ(1–42) monomer (50 μM) in 10 mM Tris, 150 mM NaCl, pH 8.0 at 37°C for 2–4 days. The samples were spun at 19000g for 10 min, and the pellet was washed with water, resedimented, and resuspended in 10 mM Tris buffer at pH 8.0 for further use.

Aβ Aggregation Reactions

All reactions and measurements were made at room temperature unless otherwise noted. Reactions were initiated in siliconized Eppendorf tubes by incubating indicated concentrations of freshly purified Aβ monomer in buffer without agitation. Aggregation kinetic parameters were obtained by monitoring the reaction with thioflavin T and fitting fluorescence (F) data points to the sigmoidal curve in Eq. (1)[30] using Sigmaplot 10.0.

$$F = \frac{a}{1 + e^{-[(t - t_{0.5})/b]}} \quad (1)$$

In this equation t is time, a and b are fixed parameters, and $t_{0.5}$ is the time to reach half-maximal thioflavin T fluorescence. Data points were unweighted. Lag times were equal to $t_{0.5}$—2b for each fitted curve.

Circular Dichroism Spectroscopy

Circular Dichroism (CD) spectra were obtained in the far UV region with a Jasco J-810 spectropolarimeter [Jasco Inc, Easton, molecular dynamics (MD)] in continuous scan mode (260–190 nm) and a 0.1 cm path-length quartz cuvette (Hellma). The acquisition parameters were 50 nm/min with 8 s response times, 1 nm bandwidth and 0.1 nm data pitch, and data sets were averaged over three scans unless otherwise noted. Spectra of appropriate blanks (solvent alone or solvent plus P1 or P2) were subtracted from the data sets as indicated. The corrected, averaged spectra were smoothed using the "means-movement" algorithm with a convolution width of 25 in the Jasco spectra analysis program. Data were normalized to mean residue ellipticity using the equation, $[\theta] = [\theta]_{obs} \times (MRW/10lc)$, where MRW is the mean residue molecular weight of Aβ(1–42) (4513 g/mol divided by 42 residues), l is the optical path length (cm), and c is the concentration (g/cm^3).

Fluorescence Spectroscopy

Thioflavin T fluorescence measurements were performed as described previously.[28,31] Briefly, the fluorescence (F) was monitored in a microcuvette with a Cary Eclipse fluorescence spectrophotometer (Varian Inc) after 15- fold dilution of Aβ(1–42) samples into 5 mM Tris-HCl (pH 8.0) containing 5 μM thioflavin T. Continuous measurements of F were taken for 10–15 min with the excitation wavelength fixed at 450 nm, the emission fixed at 482 nm, and the excitation and emission slits set at 10 nm, and the average F value was determined. The fluorescence of solvent blanks was subtracted. Fluorescence anisotropy measurements were carried out with the same instrument fitted with an auto polarization accessory. The excitation and emission wavelengths were fixed at 280 and 308 nm, respectively, to correspond to the tyrosine residue, with slit widths set to 5 nm each. The data was converted to anisotropy (r) values using the "advanced read" program provided by the manufacturer. The data were fit to the following noncooperative single site binding equation using SigmaPlot 10.0, where r_0 and r_s are anisotropy values in the absence and saturated levels of the ligand, respectively, while L_t and P_t are the respective total ligand and Aβ(1–42) concentrations.

$$r = r_0 - \left[\frac{(r_0 - r_s)}{2P_t}\right]\left[(K_d + L_t + P_t) - \sqrt{(K_d + L_t + P_t)^2 - 4L_tP_t)}\right] \quad (2)$$

Atomic Force Microscopy

Images were obtained as described previously.[32] Briefly, the samples were incubated for 15 min on freshly cleaved mica that had been modified with 3′-(aminopropyl)triethoxysilane (APTES), and the disk was briefly washed with water then dried over dessicant before imaging. A NanoScope III controller with a Mulitmode Atomic Force Microscopy (AFM) (Veeco Instruments Inc, Chadds Ford, PA) was used for imaging by ambient tapping mode.

RESULTS AND DISCUSSION

Peptides P1 and P2 Effectively Inhibit Aβ(1–42) Aggregation

To examine the effects of the designed peptides P1 and P2 on Aβ aggregation, we coincubated Aβ(1–42) with varying concentrations of P1 and P2 in separate reactions and monitored the aggregation by thioflavin T fluorescence (Figures 3A–3C). In agreement with previous reports,[27,33] incubation of Aβ(1–42) alone at 37°C resulted in an increase in fluorescence, indicating fibril formation (Figure 3A). But in sharp contrast, the coincubated mixture of Aβ(1–42) with either a 9- or 12-fold molar excess of P1 did not show a significant increase in thioflavin T fluorescence. Even after 220 h of incubation the intensity was less than 10% of that of the control, suggesting strong inhibition (Figures 3A and 3C). Decreases in P1 concentrations to substoichiometric levels (0.3:1 and 0.1:1 molar ratios of P1 to Aβ) failed to show any significant effect on aggregation (Figures 3A and 3C). Equimolar and a 3-fold molar excess of P1 resulted in ~30 and 50% decreases in fluorescence intensities after 220 h, respectively. Similar incubations of the peptide P2 with Aβ(1–42) also inhibited aggregation, but the effects were less pronounced than those of P1 (Figure 3B). The incubation with a 12-fold molar excess of P2 resulted in an ~80% reduction in the final thioflavin T fluorescence level while a 9-fold excess showed a ~60% reduction (Figure 3C). A 3-fold excess of P2 slowed the rate of aggregation but gave only a marginal reduction in final fluorescence, while equimolar and substoichiometric concentrations of P2 did not have a significant effect on Aβ(1–42) aggregation. A preliminary analysis of the 220-h points yielded IC_{50} values of ~65 and 180 μM for P1 and P2 respectively.

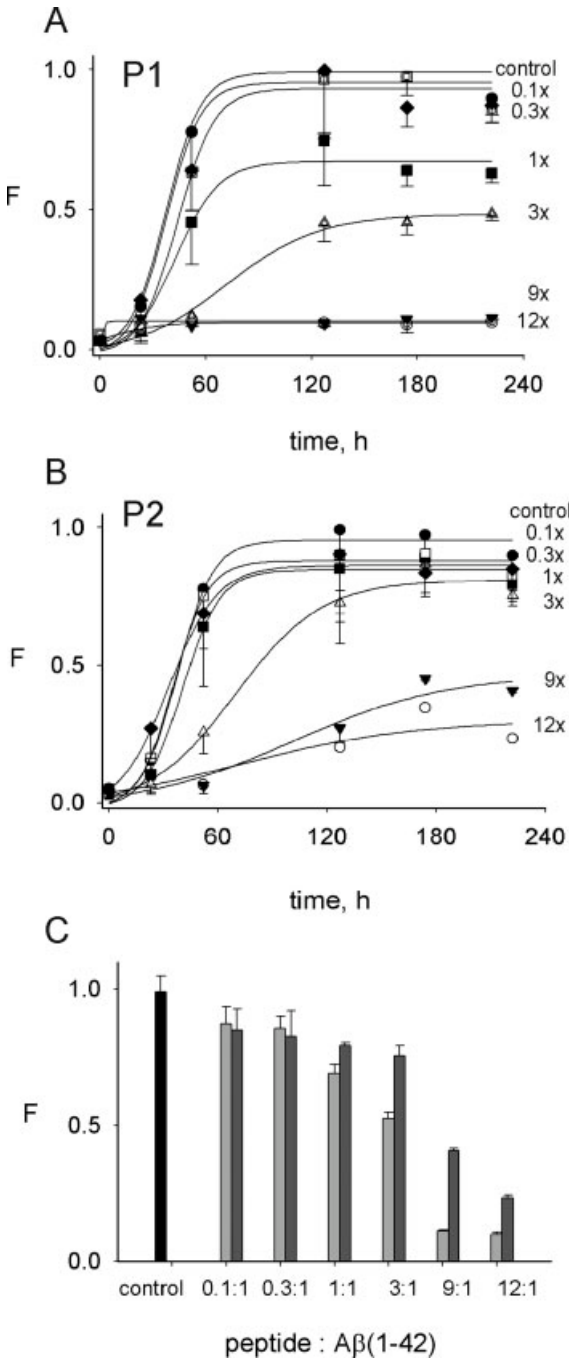

FIGURE 3 Inhibition of Aβ(1–42) aggregation by peptides P1 and P2. (A, B, and C) Dose-response curves obtained from thioflavin T assay (average of two experiments). Aβ(1–42) (25 μM) was incubated at 37°C in buffer (10 mM Tris-HCl, 50 mM NaCl, pH 8.0) alone (●), or with varying molar ratios of peptide to Aβ(1–42): (A) P1 (×12 [○], ×9 [▼], ×3 [△], ×1 [■], ×0.3 [◆] and ×0.1 [□]); B) P2 (×12 [○], ×9 [▼], ×3 [△], ×1 [■], ×0.3 [◆] and ×0.1 [□]). Aliquots were diluted 15-fold into the buffer containing thioflavin T. Fluorescence intensities F were normalized to the largest value in the reaction without P1 or P2. The solid lines are the fit of F to Eq. (1). (C) Bar graphs showing F after 222 h of incubation of Aβ(1–42) alone (black), with P1(light grey) or with P2 (dark grey).

In order to validate our design principles and rationale, we performed a series of control experiments. First, to examine the role of ΔAla residues in the inhibition of aggregation, we compared Aβ(1–42) inhibition by P1 and P2 to that of their saturated analogs P1* and P2*. In these analogs the ΔAla residues were replaced with Ala to give KLVFAIA (P1*) and KFAAAF (P2*). Thioflavin T fluorescence measurements of Aβ(1–42) aggregation with a 10-fold excess of P1 or P2 showed inhibitory effects identical to those in Figure 3 (Figure 4A). Under the same experimental conditions, P1* was essentially as effective an inhibitor as P1. Both P1 and P1* completely blocked aggregation for the first 200 h of incubation. A small increase in fluorescence was observed with P1* after 220 h that reached nearly 25% of the fluorescence of the control aggregation reaction after 390 h (Figure 4A), and a corresponding increase was not observed with P1. Aggregation experiments at a lower 3-fold excess of P1 or P1* also showed greater inhibition by P1 (data not shown). Because peptides related to the recognition sequence, KLVFF are known to inhibit Aβ aggregation,[10,12,15,17] we expected the KLVF sequence within P1* to result in P1* inhibition of aggregation to some degree. Nevertheless, the ΔAla-containing "functional motif" in P1 ultimately resulted in more effective inhibition by P1 than by P1*. The effect of the ΔAla residues in promoting inhibition of Aβ aggregation became more pronounced when the reactions with P2 and P2* were compared. P2* showed no increase in lag time and little if any reduction in the total fluorescence increase during 220 h of incubation with Aβ(1–42). In contrast, a parallel reaction with P2 indicated much more robust inhibition of the aggregation (Figure 4A), as observed previously (Figure 3B), signifying the importance of the ΔAla residues.

To further analyze the significance of ΔAla residues in the binding of P1 and P2 to Aβ, we estimated the apparent affinities of P1 and P2 for Aβ(1–42) and compared them to the affinities of their saturated counterparts. The measurements took advantage of a small increase in fluorescence anisotropy of the single tyrosine residue (Tyr10 in Aβ(1–42)) upon addition of the peptides (Figures 4B and 4C). Because fluorescence anisotropy is a function of rotational correlation times of a fluorophore, an increase in this value upon addition of a ligand will reflect the formation of a complex in which Tyr10 is more constrained. Furthermore, the increase was observed even though Tyr10 is far from the hypothesized binding domains for both P1 and P2. Titrations of Aβ(1–42) with the peptides resulted in increased anisotropy values that were fitted to a standard binding equation [see Eq. (2)]. Replicate titrations revealed reproducible qualitative binding curves for P1, P1* and P2, but no binding for P2* (Figures 4B and 4C). However, quantitative agreement of apparent dissociation constants (K_d)

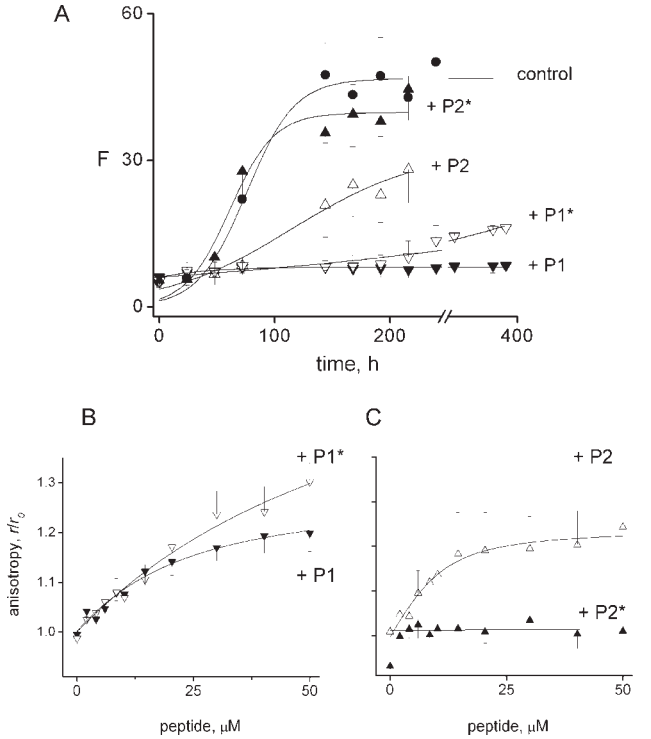

FIGURE 4 Contribution of ΔAla residues to peptide inhibition of Aβ(1–42) aggregation and to the binding of peptides to Aβ(1–42). (A) Aβ(1–42) aggregation in the presence of P1, P2, and their alanine analogs, P1* and P2*. Aβ(1–42) (25 μM) was incubated at 37°C in buffer (10 mM Tris-HCl, 20 mM NaCl, pH 8.0) alone (●), or with 250 μM P1(▼), P1* (▽), P2(△) or P2* (▲). (B and C) Peptide binding was estimated by measuring fluorescence anisotropy of tyrosine in Aβ(1–42) as a function of increasing peptide concentration. Aliquots of mixtures of 10 μM Aβ(1–42) and 100 μM peptide P1(▼) or P1* (▽) (B), and P2(△) or P2* (▲) (C) in 20 mM Tris-HCl, pH 8.0 were added to 10 μM Aβ(1–42) in the same buffer. Anisotropy values after each addition were measured in quadruplicate, and average values were fit to a standard binding equation [see Eq. (2)]. Replicate titrations revealed a slight discontinuity between average values prior to peptide addition and values at the lowest P2* concentrations, so all titrations were fit without the points at zero peptide concentration. Values of r/r_0 were calculated from each titration, and these values were then averaged for n replicate titrations ($n = 4$ for P1 and $n = 3$ for P1*, P2, and P2*). Replicate averages were then fitted to Eq. (2) to obtain apparent dissociation constant (K_d) estimates of 17 ± 8 μM for P1, 62 ± 40 μM for P1*, and 3 ± 2 μM for P2. No binding was observed for P2*. Error bars indicate replicate standard errors. The overall averaged r_0 was 0.193.

was difficult to achieve because of scatter among the replicates. Most individual titrations gave K_d values between 10 and 40 μM for all three peptides, but the few falling outside this interval suggested a more appropriate conservative K_d range of 2–100 μM. The important conclusion, however, was that P1, P1*, and P2, the three peptides that showed clear inhibition of Aβ(1–42) aggregation, also bound to Aβ(1–42) monomers. P2* in contrast, the one peptide which did not inhibit aggregation, showed no binding to monomers. These data clearly illustrate the significance of ΔAla resides in inducing P2 to become an inhibitor of Aβ aggregation.

To further demonstrate that the recognition domains in P1 and P2 are necessary for interaction with Aβ, we designed and tested a compound P0 (naphthyl-ΔAΔAΔA), that lacked a recognition motif but contained a dehydroalanine functional motif similar to those present in P1 and P2. Because P0 is extremely hydrophobic, we compared inhibition of aggregation in the presence of 13% dimethylsulfoxide (DMSO) to facilitate solubility. Under these conditions, P0 showed at most a marginal degree of inhibition relative to P1 and P2, further supporting our design principles and proposed mechanisms of inhibition (Figure 5A). In addition, we examined apparent binding of the peptides to Aβ(1–42) by again measuring the fluorescence anisotropy (Figure 5B). Absolute changes in anisotropy values were somewhat larger in the absence of DMSO (Figures 4B and 4C), indicating an effect of solvent on Tyr10 mobility. Nevertheless, fitting the data to Eq. (2) gave low micromolar K_d estimates for P1 and P2. Like P2* in Figure 4, P0 behaved as a negative control and gave no increase in anisotropy under identical titration conditions (Figure 5B).

Although thioflavin T is a useful indicator of amyloid aggregate formation, this assay can sometimes be misleading. For example, an added compound may simply compete with thioflavin T for a binding site on amyloid without inhibiting amyloid formation. We therefore used far-UV circular dichroism (CD) and AFM as complementary techniques to make additional assessments of peptide inhibition of Aβ(1–42) aggregation (see Figure 6). First, we examined the secondary structure of Aβ(1–42) in the absence and presence of the peptides by CD spectroscopy (Figures 6A and 6B). Monomeric Aβ(1–42) showed a spectrum that is characteristic of a natively unfolded or random coil structure with a negative minimum at $\lambda = 198$ nm (0 h; Figure 6A). The spectra of Aβ(1–42) with P1 and P2 also showed predominantly a random coil structure immediately after incubation (Figure 6A). After aggregation for ~10 days, Aβ(1–42) was converted from the random coil to a β-structure (negative minimum at $\lambda = 218$ nm) consistent with a fibrillar state (Figure 6B), as we observed previously.[27] However, in the presence of a 12-fold molar excess of P1, a concentration where we saw strong inhibition by thioflavin T fluorescence, the spectrum remained consistent with a predominant random coil structure even after the ~10-day incubation (Figure 6B). Although the molar ellipticity value for the spectrum was less than that for monomeric Aβ(1–42), it suggested that P1 was able to inhibit Aβ(1–42) at an early stage of aggrega-

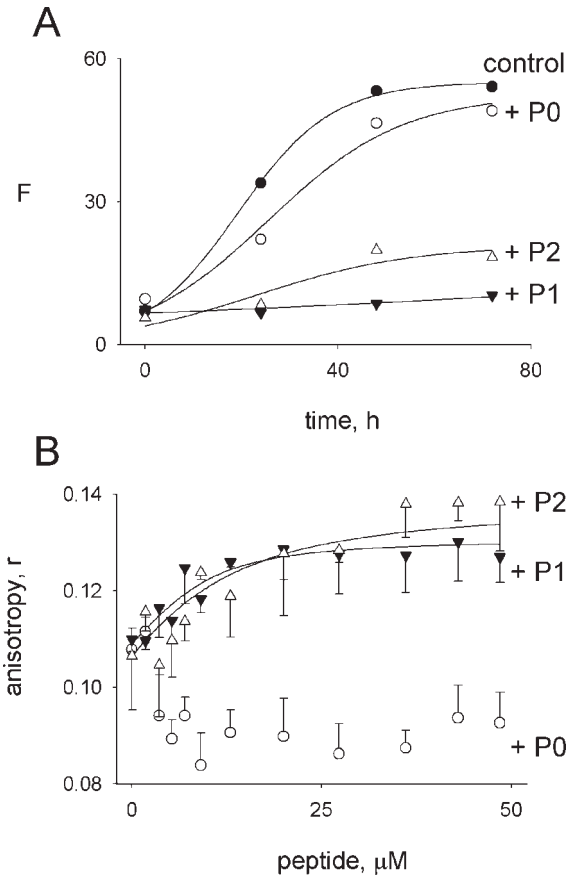

FIGURE 5 (A) Aβ(1–42) aggregation in the presence of P1, P2, and a negative control, P0. Aβ(1–42) (25 μM) was incubated at 37°C in buffer (13% DMSO, 10 mM Tris-HCl, 50 mM NaCl, pH 8.0) alone (●), or with 200 μM P0 (○), P1(▼) or P2(△). (B) Apparent binding affinity was estimated by measuring fluorescence anisotropy of tyrosine in Aβ(1–42). Aliquots of mixtures of 10 μM Aβ(1–42) and 100 μM peptide P0 (○), P1(▼) or P2(△) in the buffer in Panel A were added to 10 μM Aβ(1–42) in this buffer. Anisotropy values after each addition from two titrations were averaged and fit to Eq. (2) to give K_d estimates of 3 ± 1 μM for P1 and 7 ± 2 μM for P2. No anisotropy increase indicative of binding was observed for P0.

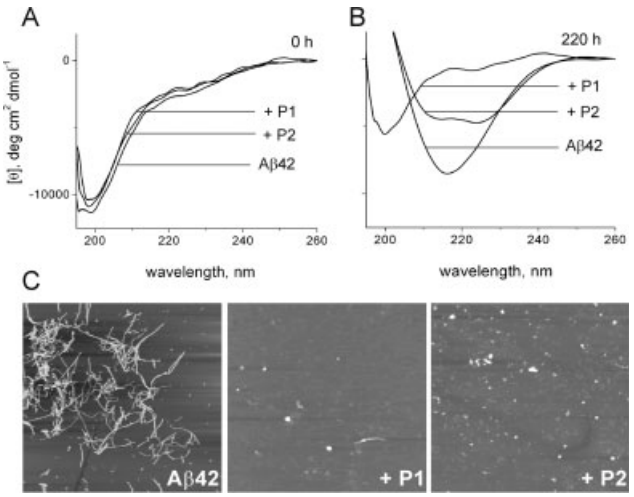

FIGURE 6 (A and B) Far-UV CD spectra were recorded for the 12-fold excess reactions in Figure 3A and B after 0 h and 220 h of incubation. Blank spectra were subtracted and curves were smoothed. For samples with P1 and P2, blanks included spectra of the respective peptides alone and were of very low amplitude (data not shown). (C) Atomic force microscopy (AFM) images following incubation of Aβ(1–42) in the absence and presence of peptides P1 and P2. Aliquots of the samples from Figure 3 after 10 days of incubation (12x molar ratio) were diluted 100-fold with water, and 150 μl was applied to the mica disks. Each panel represents a 5 × 5 μm image. The control image of Aβ(1–42) fibrils after 240 h of incubation is representative but not from the reaction in Figure 3. AFM images of the peptides P1 and P2 alone failed to show any fibrillar material (data not shown).

tion, an observation that seem to complement the thioflavin T analysis. A similar incubation of P2 after 10 days with Aβ(1–42) displayed a spectrum that was largely β-sheet but with an intensity lower than that for the control Aβ(1–42) (Figure 6B), suggesting that P2 was able to maintain Aβ(1–42) in an intermediate form that neither converted to mature fibrils nor remained as a random coil. In addition, a small shoulder at 222 nm in this spectrum indicated the presence of a low percentage of α-helical conformation not found in fibrils, providing a further structural basis for the inhibitory effect. Alternatively, the absence of a minimum at 208 nm in this spectrum could indicate a turn conformation in the complex. Nevertheless, P2 seemed to inhibit Aβ(1–42) conversion to a β-structure to a much lesser extent than P1, which again was consistent with the thioflavin T data. The peptides P1 and P2 alone remained largely as unstructured random coils throughout the incubation period, and only marginal conformational changes were observed even after several days of incubation (Supporting Information Figure S1). We next used AFM to examine the morphology of aggregates formed in the samples incubated for 10 days in Figure 3 (Figure 6C). Aβ(1–42) in the absence of the peptides showed numerous fibrillar structures, while samples with P1 and P2 (12-fold molar excess) contained few if any fibrils. Only sparsely populated spherical particles were observed with P1 consistent with the low thioflavin T fluorescence and random coil structure by CD. The sample with P2 showed globular, punctuate particles that were bigger and more numerous than those observed with P1. These CD and AFM data support the results obtained from thioflavin T fluorescence, which suggest that P1 may inhibit Aβ(1–42) aggregation at an early stage while P2 inhibits at a later stage in the aggregation pathway.

The data presented here demonstrate the overall ability of both P1 and P2 to inhibit Aβ(1–42) aggregation. Based on

the final intensities from our thioflavin T measurements, 50% inhibition of aggregation occurred at peptide: Aβ(1–42) molar ratios of ~3:1 and 5:1 for P1 and P2 respectively, and 9- to 12-fold molar excess inhibited up to 90% of the aggregation. The IC_{50} values we obtained (60 and 180 μM for P1 and P2, respectively) are significantly lower than some reported previously for peptide inhibitors of Aβ aggregation. The β-sheet breaker peptides iAβ1 and iAβ5 required a 20-fold molar excess to inhibit ~75% of Aβ(1–42) aggregation,[9,36] while the N-methylated peptides Aβ16–22m and Aβ16–22mR required 30- and 50-fold molar excess respectively to inhibit >90% of Aβ(1–40) aggregation.[12]

The P1 and P2 peptides were designed to interact with different regions of Aβ and therefore may act via distinct mechanisms. The peptide P1 was designed to target the turn conformation between residues 23 and 29 by inducing it to form an extended conformation. The persistence of a random coil conformation when Aβ(1–42) was incubated with P1 suggested that P1 may have inhibited aggregation at an early stage. However, attempts to examine the inhibition with P1 by other methods such as dynamic light scattering and SDS-PAGE were confounded by the appearance of some larger aggregates in the coincubated samples along with the monomeric Aβ(1–42) (data not shown). Therefore, inhibition at an early stage of aggregation could not be confirmed by these methods. On the other hand, P2 does seem to inhibit a later step in Aβ(1–42) aggregation, based on the greater extent of thioflavin T fluorescence and β-sheet secondary structure generated with P2 than with P1. In addition, the presence of numerous globular particles and the absence of fibrils in AFM images (Figure 5C) suggest that P2 may have trapped an intermediate Aβ aggregate.

No evidence of covalent bond formation between Aβ and ΔAla containing peptides

We selected and designed ΔAla containing pseudopeptides to provide constraints on secondary structure, and we anticipated that interactions between Aβ and ΔAla-containing peptides would be purely noncovalent. However, a ΔAla residue is a conjugated system that might be prone to nucleophilic attack on its side-chain β-carbon (1 → 4 Michael addition). Indeed, ΔAla residues have been shown to undergo such nucleophilic additions as well as to scavenge free radicals, effectively indicating their reactivity.[34,35] To eliminate the possibility that the side chains of Met, Ser or Lys residues in Aβ could act as potential nucleophiles, we investigated samples of Aβ incubated with P1 and P2 by mass spectrometry (both MALDI-TOF and ESI). Our analyses of the coincubated samples did not reveal any covalently attached complex even after 9 days of incubation (data not shown).

CONCLUSIONS

The data presented here clearly demonstrates the ability of novel ΔAla-containing peptides to interact with Aβ and suggests that different regions of Aβ may be targeted selectively. More structural evidence is required to consolidate the proposed mechanism and to further improve our designs. Experiments are currently underway to address these and will be reported elsewhere. Nevertheless, it is clear that these peptides can serve as crucial molecular tools, not only in developing therapeutic molecules for treatment of AD but also in understanding the mechanisms of Aβ amyloidogenesis. It should also be noted that the potential use of ΔAla-containing peptides as anti-amyloid compounds for many other protein misfolding diseases remains to be explored.

The authors express gratitude to Dana Kim Reed and Nicole Milkovic for their help in collecting initial AFM images and in some other experiments.

REFERENCES

1. Selkoe, D. J. Physiol Rev 2001, 81, 741–766.
2. Nilsberth, C.; Westlind-Danielsson, A.; Eckman, C. B.; Condron, M. M.; Axelman, K.; Forsell, C.; Stenh, C.; Luthman, J.; Teplow, D. B.; Younkin, S. G.; Naslund, J.; Lannfelt, L. Nat Neurosci 2001, 4, 887–893.
3. Selkoe, D. J.; Podlisny, M. B. Annu Rev Genomics Hum Genet 2002, 3, 67–99.
4. Hardy, J.; Selkoe, D. J. Science 2002, 297, 353–356.
5. Lesne, S.; Koh, M. T.; Kotilinek, L.; Kayed, R.; Glabe, C. G.; Yang, A.; Gallagher, M.; Ashe, K. H. Nature 2006, 440, 352–357.
6. Kawarabayashi, T.; Shoji, M.; Younkin, L. H.; Wen-Lang, L.; Dickson, D. W.; Murakami, T.; Matsubara, E.; Abe, K.; Ashe, K. H.; Younkin, S. G. J Neurosci 2004, 24, 3801–3809.
7. Klein, W. L.; Stine, W. B., Jr.; Teplow, D B. Neurobiol Aging 2004, 25, 569–580.
8. Sillerud, L. O.; Larson, R. S. Curr Protein Pept Sci 2005, 6, 151–169.
9. Soto, C.; Sigurdsson, E. M.; Morelli, L.; Kumar, R. A.; Castano, E. M.; Frangione, B. Nat Med 1998, 4, 822–826.
10. Findeis, M. A.; Musso, G. M.; Arico-Muendel, C. C.; Benjamin, H. W.; Hundal, A. M.; Lee, J. J.; Chin, J.; Kelley, M.; Wakefield, J.; Hayward, N. J.; Molineaux, S. M. Biochemistry 1999, 38, 6791–6800.
11. Pallitto, M. M.; Ghanta, J.; Heinzelman, P.; Kiessling, L. L.; Murphy, R. M. Biochemistry 1999, 38, 3570–3578.
12. Gordon, D. J.; Sciarretta, K. L.; Meredith, S. C. Biochemistry 2001, 40, 8237–8245.
13. Kwak, J. W.; Kim, H. K.; Chae, C. B. J Med Chem 2006, 49, 4813–4817.
14. Sato, T.; Kienlen-Campard, P.; Ahmed, M.; Liu, W.; Li, H.; Elliott, J. I.; Aimoto, S.; Constantinescu, S. N.; Octave, J. N.; Smith, S. O. Biochemistry 2006, 45, 5503–5516.
15. Tjernberg, L. O.; Lilliehook, C.; Callaway, D. J.; Naslund, J.; Hahne, S.; Thyberg, J.; Terenius, L.; Nordstedt, C. J Biol Chem 1997, 272, 12601–12605.

16. Tjernberg, L. O.; Naslund, J.; Lindqvist, F.; Johansson, J.; Karlstrom, A. R.; Thyberg, J.; Terenius, L.; Nordstedt, C. J Biol Chem 1996, 271, 8545–8548.
17. Moss, M. A.; Nichols, M. R.; Reed, D. K.; Hoh, J. H.; Rosenberry, T. L. Mol Pharmacol 2003, 64, 1160–1168.
18. Gross, E.; Morell, J. L. J Am Chem Soc 1967, 89, 2791–2792.
19. Pascard, C.; Ducruix, A.; Lunel, J.; Prange, T. J Am Chem Soc 1977, 99, 6418–6423.
20. Singh, T. P.; Kaur, P. Prog Biophys Mol Biol 1996, 66, 141–165.
21. Bhatnagar, S.; Rao, G. S.; Singh, T. P. Biosystems 1995, 34, 143–148.
22. Crisma, M.; Formaggio, F.; Toniolo, C.; Yoshikawa, T.; Wakamiya, T. J Am Chem Soc 1999, 121, 3272–3278.
23. Siddiqui, M. I.; Kataria, S.; Ahuja, V.; Rao, G. S. Indian J Biochem Biophys 2001, 38, 90–95.
24. Bhatnagar, S.; Rao, G. S. J Biomol Struct Dyn 2000, 17, 957–964.
25. Dey, S.; Vijayaraghavan, R.; Goel, V. K.; Kumar, S.; Kumar, P.; Singh, T. P. J Mol Struct 2005, 737, 109–116.
26. Petkova, A. T.; Ishii, Y.; Balbach, J. J.; Antzutkin, O. N.; Leapman, R. D.; Delaglio, F.; Tycko, R. Proc Natl Acad Sci USA 2002, 99, 16742–16747.
27. Rangachari, V.; Moore, B. D.; Reed, D. K.; Bridges, A. W.; Conboy, E.; Hartigan, D.; Rosenberry, T. L. Biochemistry 2007, 46, 12451–12462.
28. Nichols, M. R.; Moss, M. A.; Reed, D. K.; Lin, W. L.; Mukhopadhyay, R.; Hoh, J. H.; Rosenberry, T. L. Biochemistry 2002, 41, 6115–6127.
29. Fezoui, Y.; Hartley, D. M.; Harper, J. D.; Khurana, R.; Walsh, D. M.; Condron, M. M.; Selkoe, D. J.; Lansbury, P. T., Jr.; Fink, A. L.; Teplow, D. B. Amyloid 2000, 7, 166–178.
30. Nielsen, L.; Khurana, R.; Coats, A.; Frokjaer, S.; Brange, J.; Vyas, S.; Uversky, V. N.; Fink, A. L. Biochemistry, 2001, 40, 8397–8409.
31. LeVine, H, III. Protein Sci 1993, 2, 404–410.
32. Nichols, M. R.; Moss, M. A.; Reed, D. K.; Hoh, J. H.; Rosenberry, T. L. Microsc Res Tech 2005, 67, 164–174.
33. Naiki, H.; Hasegawa, K.; Yamaguchi, I.; Nakamura, H.; Gejyo, F.; Nakakuki, K. Biochemistry 1998, 37, 17882–17889.
34. Breukink, E.; de Kruijff, B. Nat Rev Drug Discov 2006, 5, 321–332.
35. Buc-Calderon, P.; Praet, M.; Ruysschaert, J. M.; Roberfroid, M. Eur J Cancer Clin Oncol 1989, 25, 679–685.
36. Soto, C.; Kindy, M. S.; Baumann, M.; Frangione, B. Biochem Biophys Res Commun 1996, 226, 672–680.

Reviewing Editor: Alfred Wittinghofer